

# Hydrothermal Synthesis, Crystal Structure and Characterization of a Microporous 3D Pillared-Layer 3d–4f Copper–Holmium Heterometallic Coordination Polymer

Le-Qing Fan,\* Ji-Huai Wu, Yun-Fang Huang, Jian-Ming Lin, and Yue-Lin Wei

Engineering Research Center of Environment-Friendly Functional Materials, Ministry of Education, College of Materials Science and Engineering, Huaqiao University, Xiamen, Fujian 361021, P.R. China

\*E-mail: lqfan@hqu.edu.cn

Received December 23, 2013, Accepted February 8, 2014

**Key Words** : 3d–4f, Heterometallic coordination polymer, Microporous, Magnetic properties

There has been more and more interest in recent years in the design and synthesis of porous coordination polymers (PCPs) not only for their fascinating structural diversity but also for their potential applications as functional materials in magnetism, molecular adsorption, gas storage, ion exchange, catalysis and separation.<sup>1</sup> Up to now, almost all approaches to the construction of porous materials have focused on the 3D monometallic PCPs. However, the preparation of heterometallic PCPs especially containing lanthanide (Ln) and transition metal (TM) ions has been drawn less attention.<sup>2</sup> A pillared-layer approach to the construction of 3D 3d–4f coordination polymers upon the connections of Ln-carboxylate layers and TM-inorganic motifs by organic pillars *via* coordination bonding has been reported.<sup>3</sup> In most such 3D pillared-layer 3d–4f structures, TM-inorganic layers/chains generally obstruct the development of channels based on the pores formed by Ln-carboxylate layers. However, Yang *et al.* reported the first 3D pillared-layer Ln–Cu PCPs which were obtained in the presence of I<sup>−</sup> having high coordination numbers and versatile coordination modes, demonstrating that under appropriate synthesis conditions the 3D 3d–4f PCPs can be prepared through the pillared-layer approach.<sup>3a</sup> On the other hand, it is found that, in many complexes, Br<sup>−</sup> ions can act as  $\mu_4$ -,  $\mu_3$ - and  $\mu_2$ -bridging ligands.<sup>4</sup> So, in view of the similarity between Br<sup>−</sup> and I<sup>−</sup> ions, the formation of such 3D pillared-layer Ln–Cu PCPs based on the linkages of Cu–Br inorganic motifs and Ln-carboxylate layers by organic pillars may become true.

In this paper, we report the synthesis, crystal structure and characterization of a 3D pillared-layer 3d–4f (Cu<sup>+</sup>–Ho<sup>3+</sup>) PCP, {Ho<sub>2</sub>Cu<sub>4</sub>Br<sub>4</sub>(IN)<sub>4</sub>(OAc)<sub>2</sub>(H<sub>2</sub>O)<sub>2</sub>·H<sub>2</sub>O}<sub>n</sub> (**1**) (HOAc = acetic acid), which is constructed upon on the linkages of 2D wavelike Ho-carboxylate layers and 1D Cu<sub>4</sub>Br<sub>4</sub> inorganic chains in centipede-type structure by IN<sup>−</sup> pillars.

## Experimental Section

**Materials and Characterization Methods.** All of the reagent-grade reactants were commercially available and employed without further purification. Powder X-ray diffraction (PXRD) datum was measured on a DMAX2500 diffractometer. Solid infrared (IR) spectrum was obtained from a

Nicolet Nexus 470 FT-IR spectrometer between 400 and 4000 cm<sup>−1</sup> using KBr pellet. Element analyses of carbon, hydrogen and nitrogen were performed with a Vario EL III element analyzer. Thermogravimetric analysis (TGA) was performed on a Netzsch Sta449C thermoanalyzer under N<sub>2</sub> atmosphere in the range of 30–600 °C at a heating rate of 10 °C/min. Variable-temperature magnetic susceptibilities were performed with a PPMS-9T magnetometer over the temperature range of 2–300 K under a magnetic field of 1000 Oe. A diamagnetic correction was estimated from Pascal's constants.<sup>5</sup> The crystal structure was determined by a Rigaku Mercury CCD area-detector diffractometer and SHELXL crystallographic software of molecular structure.

**Synthesis of {Ho<sub>2</sub>Cu<sub>4</sub>Br<sub>4</sub>(IN)<sub>4</sub>(OAc)<sub>2</sub>(H<sub>2</sub>O)<sub>2</sub>·H<sub>2</sub>O}<sub>n</sub> (**1**).** A mixture of Ho<sub>2</sub>O<sub>3</sub> (0.189 g, 0.5 mmol), CuBr<sub>2</sub> (0.223 g, 1 mmol), HIN (0.246 g, 2 mmol), malonate (0.208 g, 2 mmol) and H<sub>2</sub>O (10 mL) was stirred at room temperature until a homogeneous mixture was obtained. The mixture was transferred into a Teflon-line autoclave (23 mL) and heated at 170 °C for 7 days and then cooled at rate of 2 °C h<sup>−1</sup> to room temperature. Yellow block crystals of **1** were recovered by filtration, washed with distilled water, and dried in air (36% yield based on Ho). Anal. Calcd. for **1** (dried) (%): C, 21.50; H, 1.80; N, 3.58. Found: C, 21.63; H, 1.91; N, 3.37. Selected IR data (KBr pellet, cm<sup>−1</sup>): 3463, 1621, 1540, 1412, 769, 688. PXRD pattern for the bulk product is in fair agreement with the pattern based on single-crystal X-ray solution in position, indicating the phase purity of the as-synthesized sample of **1** (Figure S1). The difference in reflection intensities between the simulated and experimental patterns was due to the variation in preferred orientation of the powder sample during collection of the experimental PXRD data.

**X-ray Crystal Determination.** The crystallographic data for **1** were collected on a Rigaku Mercury CCD area-detector equipped with a graphite-monochromated MoK $\alpha$  radiation ( $\lambda = 0.71073$  Å) at 293(2) K using an  $\omega$ -2 $\theta$  scan mode. Absorption correction was performed by the CrystalClear program.<sup>6</sup> This structure was solved by direct methods using SHELXS-97 program and refined by full-matrix least-squares refinement on  $F^2$  with the aid of SHELXL-97 program.<sup>7</sup> All non-hydrogen atoms were refined anisotropically. Hydrogen atoms attached to carbon were placed in geo-

metrically idealized positions and refined using a riding model. Hydrogen atoms on water molecules were located from difference Fourier maps and were also refined using a riding model. The Cu(2) and Br(2) atoms in **1** are disordered, and occupy 74.3% and 83.5% of the corresponding sites, respectively. Some refinement details and crystal data of **1** are summarized in Table S1. Selected bond lengths and bond angles of **1** are shown in Table S2.

## Results and Discussion

The compound **1** was synthesized from the reaction mixture of  $\text{Ho}_2\text{O}_3$ ,  $\text{CuBr}_2$ , HIN and malonate with the mole ratio of 1:2:4:4 in water at 170 °C by the hydrothermal technique. And it was found that crystals suitable for X-ray single-crystal analysis were obtained only with this ratio. However, isomorphous compounds with other  $\text{Ln}^{3+}$  having larger or smaller ion radii are not obtained. Series of experiments using  $\text{Cl}^-$  and  $\text{I}^-$  ions as halide sources in place of  $\text{Br}^-$  ion have been carried out to prepare compounds similarly structural to this compound, but unfortunately, we were unsuccessful. The main reason may be that  $\text{Cl}^-$  and  $\text{I}^-$  have smaller and larger ion radii than  $\text{Br}^-$ , respectively, which do not favor proper coordination numbers that benefit to give rise to such a microporous 3D pillared-layer network. On the other hand, during the hydrothermal reaction, *in-situ* decarboxylation of malonate gives  $\text{OAc}^-$  ligand. So, experiments using  $\text{NaOAc}$  instead of malonate have been carried out to prepare the compound **1** and isomorphous compounds with other  $\text{Ln}^{3+}$ . But no crystal was produced. It is suggested that the reaction condition was changed for replacement of malonate by  $\text{NaOAc}$ .

Single crystal X-ray diffraction study revealed that **1** is a 3D pillared-layer PCP based on the linkages of 2D Ho-carboxylate layers and 1D  $\text{Cu}_4\text{Br}_4$  inorganic chains by  $\text{IN}^-$  pillars. An ORTEP view of **1** is shown in Figure 1. The asymmetric unit of **1** contains one unique  $\text{Ho}^{3+}$  ion, two (1 + 0.5 + 0.5)  $\text{Cu}^+$  ions, two (1 + 0.5 + 0.5)  $\text{Br}^-$  ions, two  $\text{IN}^-$  ligands, one  $\text{OAc}^-$  ligand, one coordinated water molecule and half an uncoordinated water molecule. Ho(1) center is eight-coordinated and displays distorted bicapped trigonal-prism coordination environment: four oxygen atoms from four  $\text{IN}^-$  ligands, three oxygen atoms from two  $\text{OAc}^-$  ligands, one oxygen atom from coordinated water molecule. The Ho–O bond lengths vary from 2.299(4) to 2.463(4) Å, and the O–Ho–O bond angles are in the range of 53.78(14)–153.99(14)°, thus being in the normal range observed in other compounds.<sup>8</sup> Cu(1) center exhibits tetrahedral conformation, being coordinated by one nitrogen atom from  $\text{IN}^-$  ligand and three  $\text{Br}^-$  ions. But, Cu(2) and Cu(3) centers present trigonal geometry: two nitrogen atoms from two  $\text{IN}^-$  ligands and one  $\text{Br}^-$  ion for Cu(2); three  $\text{Br}^-$  ions for Cu(3). The Cu–N bond lengths are 2.038(5) and 1.955(6) Å, and Cu–Br bond lengths range from 2.372(2) to 2.8256(15) Å, all within the range of those observed for other Ln–Cu compounds.<sup>9</sup> In this structure, the  $\text{IN}^-$  ligand has only one coordination mode: behaving as a bridging ligand to coordi-

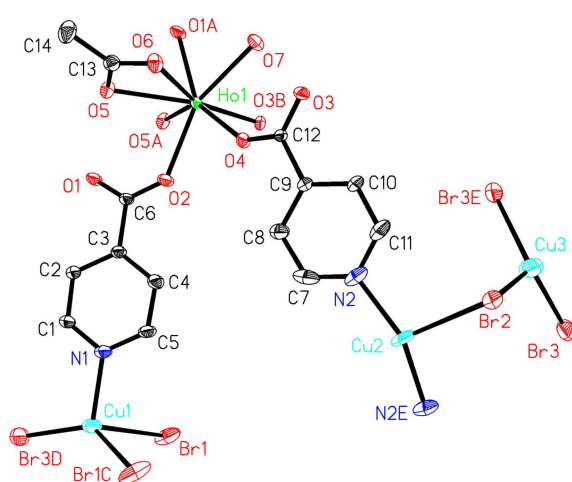


**Figure 1.** ORTEP plot of the asymmetric unit of **1** (30% probability ellipsoids). All H atoms and uncoordinated water molecule are omitted for clarity. Symmetry codes: A =  $-x, 1 - y, 1 - z$ ; B =  $-1/2 + x, y, 3/2 - z$ ; C =  $1/2 + x, y, 1/2 - z$ ; D =  $x, 3/2 - y, -1 + z$ ; E =  $x, 3/2 - y, z$ .

nate two  $\text{Ho}^{3+}$  ions and one  $\text{Cu}^+$  ion (Scheme S1a). The  $\text{OAc}^-$  ligand also has only one coordination mode: acting as a bridging ligand to coordinate two  $\text{Ho}^{3+}$  ions (Scheme S1b). It is noted that the  $\text{OAc}^-$  ligand came from the *in-situ* decarboxylation of malonate in the hydrothermal reaction. The decarboxylation reaction in the transformation of 2,5-pyridinedicarboxylic acid into nicotinic acid was also found in the preparation of Ln–Cu coordination polymer under hydrothermal condition.<sup>10</sup> The reason may be that pressure under hydrothermal condition is a necessary factor for the decarboxylation reaction. Although  $\text{Cu}^{2+}$  ions were used as starting materials in **1**, the Cu centers have an oxidation state of +1, attributed to a reduction reaction involving the  $\text{IN}^-$  ligands,<sup>9a,11</sup> and is consistent with the geometry of the  $\text{Cu}^+$  ions and evidenced by the yellow color of crystals.

Two Ho(1) centers are connected by four carboxylate groups from two different  $\text{IN}^-$  ligands and two different  $\text{OAc}^-$  ligands to form  $\text{Ho}_2$  dinuclear unit with Ho···Ho distance of 3.8361(5) Å (Figure 2). Adjacent  $\text{Ho}_2$  dinuclear units are bridged by four  $\text{IN}^-$  ligands to produce novel 2D wavelike Ho-carboxylate layers extending along *ac* plane (Figure S2 and Figure S3). As shown in Figure 3(a), two adjacent Cu(1) $\text{Br}_3\text{N}$  tetrahedra are connected by common edge (Br(1)–Br(1)) to form a  $\text{Cu}_2\text{Br}_4\text{N}_2$  dimer, which further links one Cu(3) $\text{Br}_3$  triangle through sharing vertices (Br(3)) to generate  $\text{Cu}_3\text{Br}_5\text{N}_2$  trimer, where Cu(1)–Cu(1) and Cu(1)–Cu(3) distances are 2.8805(19) and 2.7549(17) Å, respectively, which is comparable with the double van der Waals radius of the  $\text{Cu}^+$  ion (1.4 Å), implying relatively strong Cu–Cu interactions. The phenomena of Cu–Cu interactions have been observed for other Ln–Cu compounds.<sup>9b,12</sup> The  $\text{Cu}_3\text{Br}_5\text{N}_2$  trimer joins Cu(2) $\text{Br}_3\text{N}_2$  triangle via sharing vertex (Br(2)) to engender  $\text{Cu}_4\text{Br}_5\text{N}_4$  tetramer. Neighboring  $\text{Cu}_4\text{Br}_5\text{N}_4$  tetramers link each other by common vertices (Br(1)) to form unusual 1D  $\text{Cu}_4\text{Br}_4$  inorganic chains in centipede-type structure along *a* axis (Figure 3(b)). As a consequence of the

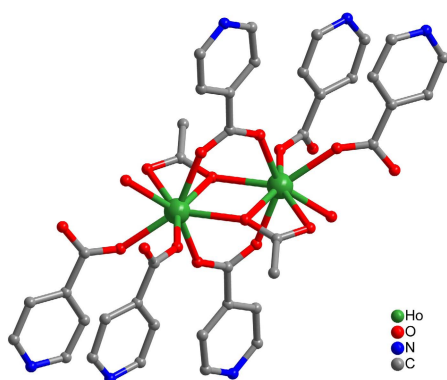


Figure 2. Diagram of Ho<sub>2</sub> dinuclear unit.

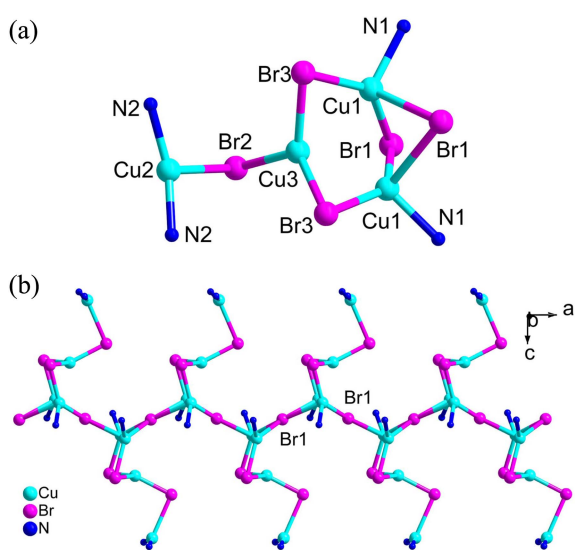


Figure 3. (a) Diagram of Cu<sub>4</sub>Br<sub>5</sub>N<sub>4</sub> tetramer. (b) Diagram of 1D Cu<sub>4</sub>Br<sub>4</sub> inorganic chain in centipede-type structure.

connectivity of CuBr<sub>3</sub>N tetrahedral, and CuBr<sub>3</sub> and CuBrN<sub>2</sub> triangles in **1**, the Br<sup>-</sup> ions act as  $\mu_2$  (Br(2), Br(3)) and  $\mu_4$  (Br(1)) ligands. 2D Ho-carboxylate layers and 1D Cu<sub>4</sub>Br<sub>4</sub> inorganic chains are connected by IN<sup>-</sup> pillars to give birth to such a novel 3D pillared-layer network (Figure S4), which contains 1D channels with dimensions of about  $7.5 \times 11.6$  Å (based on Ho $\cdots$ Ho separations) along the *b* axis (Figure 4), providing an example of microporous 3D pillared-layer 3d-4f coordination polymer. As shown in Figure 4, the channels in **1** impenate not only Ho-carboxylate layers but also Cu-Br inorganic chains almost locating at a plane, which benefits from the peculiar centipede-type structure of the latter. The uncoordinated water molecules situate in the channels by O-H $\cdots$ Br hydrogen bondings (Table S3).

In the IR spectrum of **1** (Figure S5), the strong and broad absorption band in the range of about  $3463\text{ cm}^{-1}$  is assigned as characteristic peak of OH vibration. The strong vibrations appearing at  $1621$  and  $1412\text{ cm}^{-1}$  correspond to the asymmetric and symmetric stretching vibrations of carboxylate group, respectively. The absence of strong bands in the range of  $1690\text{--}1730\text{ cm}^{-1}$  indicates that all carboxyl groups of HIN are deprotonated.<sup>13</sup>

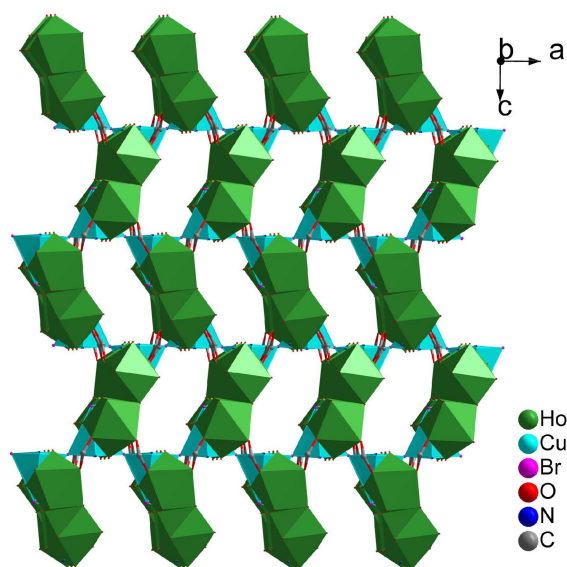


Figure 4. Polyhedral diagram of **1** viewed approximately down the [010] direction. All uncoordinated water molecules, and IN<sup>-</sup> and OAc<sup>-</sup> ligands are omitted for clarity.

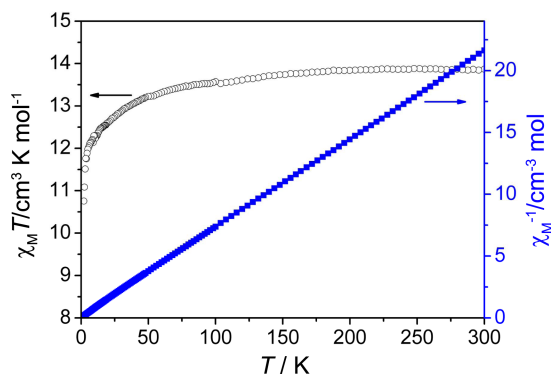


Figure 5. Plots of  $\chi_M^{-1}$  (■) and  $\chi_M T$  (○) vs. *T* of **1** over the temperature of 2–300 K at the field of 1000 Oe.

To study the thermal stability of **1**, TGA was performed on polycrystalline sample of this complex in N<sub>2</sub> atmosphere from 30 to 600 °C (Figure S6). The lattice-water and coordinated water molecules are gradually lost in the temperature ranging 25–235 °C (calcd/found: 3.45/3.71%). Thereafter **1** is stable to *ca.* 270 °C. Above this temperature, the weight loss is due to the decomposition of the organic ligand and the collapse of the whole framework.

The magnetic susceptibilities of **1** have been measured from ground crystals under a constant magnetic field of 1000 Oe over the temperature range of 2–300 K. The data are presented as plots of  $\chi_M^{-1}$  vs. *T* and  $\chi_M T$  vs. *T* ( $\chi_M$  being molar magnetic susceptibility per Ho<sup>3+</sup> ion) in Figure 5. The observed  $\chi_M T$  at room temperature is  $13.82\text{ cm}^3\text{ K mol}^{-1}$ , which is close to the theoretical value of  $14.07\text{ cm}^3\text{ K mol}^{-1}$  on the basis of a independent Ho<sup>3+</sup> ion in the  $^5I_8$  ground state ( $g = 5/4$ ). The  $\chi_M T$  decreases slowly from room temperature to 50 K, and then decreases abruptly to  $10.78\text{ cm}^3\text{ K mol}^{-1}$  at 2 K. The  $\chi_M^{-1}$  vs. *T* plot obeys the Curie-Weiss law,  $\chi_M = C/(T-\theta)$ , over the temperature range from 2 to 300 K with

Curie constant  $C = 13.96 \text{ cm}^3 \text{ K mol}^{-1}$ , Weiss constant  $\theta = -2.17 \text{ K}$ . However, the trend of the  $\chi_M T$  value and the negative value of  $\theta$  cannot unambiguously confirm the existence of antiferromagnetic coupling between two adjacent  $\text{Ho}^{3+}$  ions because of the strong spin-orbit coupling for  $\text{Ln}^{3+}$  ions and the progressive thermal depopulation of the  $\text{Ln}^{3+}$  Stark components.<sup>14</sup>

In conclusion, a microporous 3D pillared-layer 3d-4f ( $\text{Cu}^+ - \text{Ho}^{3+}$ ) coordination polymer based on the linkages of 2D wavelike Ho-carboxylate layers and 1D  $\text{Cu}_4\text{Br}_4$  inorganic chains in centipede-type structure by  $\text{IN}^-$  pillars has been obtained. Furthermore, the magnetic properties of this complex have been investigated. Our results provide an intriguing example of 3D 3d-4f PCPs and further demonstrate that the pillared-layer approach can be used for constructing novel 3D 3d-4f PCPs.

**Supplementary Material.** Crystallographic data for the structure reported here have been deposited with CCDC (No. CCDC-954960). These data can be obtained free of charge via <http://www.ccdc.cam.ac.uk/conts/retrieving.html> or from CCDC, 12 Union Road, Cambridge CB2 1EZ, UK, E-mail: [deposit@ccdc.cam.ac.uk](mailto:deposit@ccdc.cam.ac.uk)

**Acknowledgments.** This work was supported financially by the National Natural Science Foundation of China (Nos. U1205112, 21301060, 61306077), Promotion Program for Young and Middle-aged Teacher in Science and Technology Research of Huaqiao University (No. ZQN-PY106) and the Fund of Fujian Provincial Key Laboratory of Nanomaterials (No. NM10-5).

## References

- (a) Li, J. R.; Kuppler, R. J.; Zhou, H. C. *Chem. Soc. Rev.* **2009**, *38*, 1477. (b) Chen, B.; Liang, C.; Yang, J.; Contreras, D. S.; Clancy, Y. L.; Lobkovsky, E. B.; Yaghi, O. M.; Dai, S. *Angew. Chem. Int. Ed.* **2006**, *45*, 1390. (c) Son, K. I.; Lee, H. J.; Kim, J.; Noh, D. Y. *Bull. Korean Chem. Soc.* **2012**, *33*, 2773. (d) Ma, F. J.; Liu, S. X.; Sun, C. Y.; Liang, D. D.; Ren, G. J.; Wei, F.; Chen, Y. G.; Su, Z. M. *J. Am. Chem. Soc.* **2011**, *133*, 4178. (e) Yang, T.; Cui, H.; Zhang, C.; Zhang, L.; Su, C. Y. *Inorg. Chem.* **2013**, *52*, 9053. (f) Liao, J. H.; Chen, W. T.; Tsai, C. S.; Wang, C. C. *CrysEngComm* **2013**, *15*, 3377.
- (a) Zhu, X. D.; Lin, Z. J.; Liu, T. F.; Xu, B.; Cao, R. *Cryst. Growth Des.* **2012**, *12*, 4708. (b) Wang, Y.; Fang, M.; Li, Y.; Liang, J.; Shi, W.; Chen, J.; Cheng, P. *Int. J. Hydrogen Energy* **2010**, *35*, 8166. (c) Li, C. J.; Lin, Z. J.; Peng, M. X.; Leng, J. D.; Yang, M. M.; Tong, M. L. *Chem. Commun.* **2008**, 6348. (d) Wang, F.; Yang, H.; Kang, Y.; Zhang, J. *J. Mater. Chem.* **2012**, *22*, 19732.
- (a) Cheng, J. W.; Zhang, J.; Zheng, S. T.; Yang, G. Y. *Chem. Eur. J.* **2008**, *14*, 88. (b) Gu, X.; Xue, D. *Inorg. Chem.* **2007**, *46*, 5349. (c) Li, X.; Huang, Y.; Cao, R. *Cryst. Growth Des.* **2012**, *12*, 3549. (d) Peng, G.; Liu, Z.; Ma, L.; Liang, L.; Zhang, L.; Kostakis, G. E.; Deng, H. *CrysEngComm* **2012**, *14*, 5974. (e) Cheng, J. W.; Zheng, S. T.; Ma, E.; Yang, G. Y. *Inorg. Chem.* **2007**, *46*, 10534. (f) Fan, L. Q.; Wu, J. H.; Huang, Y. F. *J. Solid State Chem.* **2011**, *184*, 2472.
- (a) Hou, J. J.; Li, S. L.; Li, C. R.; Zhang, X. M. *Dalton Trans.* **2010**, *39*, 2701. (b) Tsui, E. Y.; Day, M. W.; Agapie, T. *Angew. Chem. Int. Ed.* **2011**, *50*, 1668.
- Kahn, O. *Molecular Magnetism*; VCH: Weinheim, Germany, 1993.
- Rigaku, CrystalClear, version 1.3.6, Rigaku/MS, Tokyo, Japan, 2005.
- (a) Sheldrick, G. M. *SHELXS-97*, Program for the Solution of Crystal Structures, University of Göttingen, Germany, 1997. (b) Sheldrick, G. M. *SHELXL-97*, Program for the Refinement of Crystal Structures, University of Göttingen, Germany, 1997.
- (a) Liu, B.; Liu, Q.; Xiao, H.; Zhang, W.; Tao, R. *Dalton Trans.* **2013**, *42*, 5047. (b) Li, Z. H.; Hong, D. F.; Xue, L. P.; Fu, W. J.; Zhao, B. T. *Inorg. Chim. Acta* **2013**, *400*, 239.
- (a) Fan, L. Q.; Wu, J. H.; Huang, Y. F. *Inorg. Chem. Commun.* **2011**, *14*, 1906. (b) Cheng, J. W.; Zheng, S. T.; Yang, G. Y. *Inorg. Chem.* **2007**, *46*, 10261.
- Cheng, J. W.; Zheng, S. T.; Yang, G. Y. *Inorg. Chem.* **2008**, *47*, 4930.
- Xiao, W.; Gu, X.; Xue, D. *J. Cryst. Growth* **2009**, *311*, 601.
- (a) Gu, X.; Xue, D. *Inorg. Chem.* **2007**, *46*, 5349. (b) Li, Z. Y.; Wang, N.; Dai, J. W.; Yue, S. T.; Liu, Y. L. *CrysEngComm* **2009**, *11*, 2003.
- (a) Qiu, Y.; Liu, Z.; Mou, J.; Deng, H.; Zeller, M. *CrysEngComm* **2010**, *12*, 277. (b) Fan, L. Q.; Chen, Y.; Wu, J. H.; Huang, Y. F. *J. Solid State Chem.* **2011**, *184*, 899.
- (a) Sun, Y. G.; Wu, Y. L.; Xiong, G.; Smet, P. F.; Ding, F.; Guo, M. Y.; Zhu, M. C.; Gao, E. J.; Poelman, D.; Verpoort, F. *Dalton Trans.* **2010**, *39*, 11383. (b) Zhou, X. H.; Peng, Y. H.; Gu, Z. G.; Zuo, J. L.; You, X. Z. *Inorg. Chim. Acta* **2009**, *362*, 3447. (c) Kahn, M. L.; Sutter, J. P.; Golhen, S.; Guionneau, P.; Ouahab, L.; Kahn, O.; Chasseau, D. *J. Am. Chem. Soc.* **2000**, *122*, 3413.